Environmental Science & Technology

Article

pubs.acs.org/est

Low-Volatility Model Demonstrates Humidity Affects Environmental Toxin Deposition on Plastics at a Molecular Level

Jeanne M. Hankett,[†] William R. Collin,[†] Pei Yang,[†] Zhan Chen,*[,†] and Melissa Duhaime*[,‡]

[†]Department of Chemistry, University of Michigan, 930 North University Avenue, Ann Arbor, Michigan 48109 United States

[‡]Department of Ecology and Evolutionary Biology, University of Michigan, 830 North University Ave, Ann Arbor, Michigan 48109 United States

Supporting Information

ABSTRACT: Despite the ever-increasing prevalence of plastic debris and endocrine disrupting toxins in aquatic ecosystems, few studies describe their interactions in freshwater environments. We present a model system to investigate the deposition/desorption behaviors of low-volatility lake ecosystem toxins on microplastics in situ and in real time. Molecular interactions of gas-phase nonylphenols (NPs) with the surfaces of two common plastics, poly(styrene) and poly(ethylene terephthalate), were studied using quartz crystal microbalance and sum frequency generation vibrational spectroscopy. NP point sources were generated under two model environments: plastic on land and plastic on a freshwater surface. We found the headspace above calm water provides an excellent environment for NP deposition and demonstrate significant NP deposition on plastic within minutes at relevant concentrations. Further, NP deposits and orders differently on both plastics under humid versus dry environments. We attributed the unique deposition behaviors to surface energy changes from increased water content during the humid deposition. Lastly, nanograms of NP remained on microplastic surfaces hours after initial NP introduction and agitating conditions, illustrating feasibility for plastic-bound NPs to interact with biota and surrounding matter. Our model studies reveal important interactions between low-volatility environmental toxins and microplastics and hold potential to correlate the environmental fate of endocrine disrupting toxins in the Great Lakes with molecular behaviors.

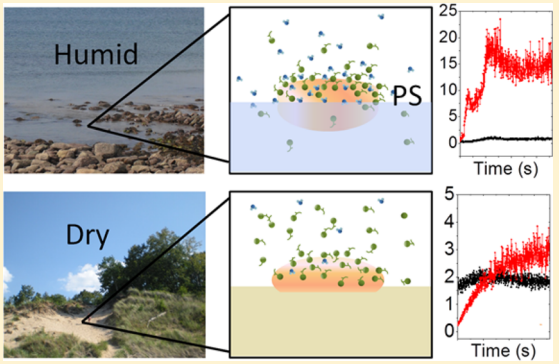

INTRODUCTION

Ubiquitous Aquatic Plastic Debris and Its Associated Toxins. Plastics are a permanent and increasingly prevalent pollutant in our freshwater ecosystems. The world's largest[1] and most remote[2] lake and fluvial[3] ecosystems contain concentrations of surface plastic debris among the highest documented in any environment. While plastic debris puts macrofauna at risk of entanglement and suffocation due to ingestion,[4] plastics also serve as vectors of hydrophobic toxins that adhere to polymer surfaces at ng-μg/g concentrations[5−7] (up to 10^6 times higher than in surrounding water[6]) with myriad implications for organismal health.[8]

Determining the potential for anthropogenic plastic pollution to adhere toxins, including endocrine disruptors and persistent organic pollutants, is of increasing focus.[9] Along with buoyant plastic debris, these toxins are at highest concentrations in the water-atmosphere interface microlayer (1−1000 μm), where they can be found at concentrations 500 times greater than in the underlying bulk water.[10] Studies of polymer-toxin interactions have found toxins to transfer from seawater to virgin plastic in days.[11] Desorption studies modeling the fate of ingested plastic-bound toxins have found transfer *off* of plastic to be 30 times greater under physiological conditions simulating a gut environment,[12] and direct transfer of toxins to biota has been shown to be significantly higher from contaminated plastics than from other contaminated food sources.[8] Yet, little is known of molecular behavior during toxin deposition, adsorption, and desorption in terms of *where*—at the molecule-scale—and *how* toxins interact with these anthropogenic sinks of environmental toxins near the water−atmosphere interface.[1,13−19]

Nonylphenols in the Environment. Positional isomers of nonylphenol (NP) are part of a class of endocrine disrupting alkylphenols manufactured at large volumes as nonionic surfactant precursors and precursors/additives for products including industrial detergents, emulsifiers, paints, lubricants, and personal care products.[20,21] NPs are categorized as suspected human reproductive toxicants and acute and chronic toxicants for aquatic organisms.[20] Industrially, no single isomer of NP is utilized for surfactant production and a mixture of isomers can be found in both manufactured products and natural environments, including aquatic ecosystems and

Received: November 13, 2015
Revised: January 4, 2016
Accepted: January 11, 2016
Published: January 11, 2016

DOI: 10.1021/acs.est.5b05598
Environ. Sci. Technol. 2016, 50, 1304−1312

agricultural and urban environments.[15,22−25] Branched isomers, similar to Figure 1, tend to dominate isomer mixtures.[26,27]

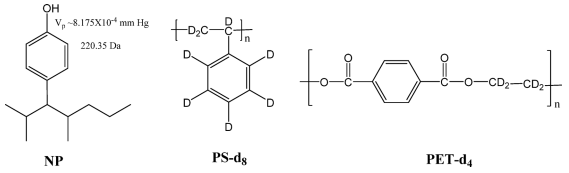

Figure 1. Molecular structure of a generic 4-nonylphenol branched isomer (left), structures of polymers used in this study: middle, deuterated poly(styrene), right, deuterated poly(ethylene terephthalate).

In 2014, due to the proliferation of NPs in natural aquatic ecosystems and their potential adverse effects on the environment, the U.S. Environmental Protection Agency added the category of nonylphenols to the Toxic Release Inventory (TRI) list of reportable chemicals, officially highlighting these molecules as a danger to aquatic organisms.[28] In addition to the new TRI categorization, NPs appear on many pharmaceuticals and personal care products indicator lists as endocrine disruptors and xenoestrogens. Ecosystems especially vulnerable are watersheds where large volumes of NPs may collect after manufacturing, production, and use.[22] Ppm levels of NP and other alkylphenol concentrations have been reported in the surface waters of the Laurentian Great Lakes as well as in and above river estuaries and in wastewaters.[22] Microplastics collected from *marine* aquatic systems have been reported to contain NP and endocrine disruptor toxins with similar polarities—and thus vapor phase behaviors—to NPs, such as phthalates, bisphenol A, and PCBs.[7,29−32] Yet, despite the known prevalence of plastics and endocrine disrupting toxins in freshwater environments, there are few studies describing their interactions in freshwater conditions.[18,33,34]

Establishing a Model System to Study Plastic−Toxin Interactions. Low-volatility alkylphenols like NPs offer great challenges to scientists studying gas-phase toxin sorption and desorption mechanics. Low air concentrations, increased equilibrium times, and deposition of molecules onto lab equipment make it difficult to collect accurate data and depict environmentally relevant situations in-house.[35] Difficulty increases when a small surface area for deposition must be studied, like that of a microplastic (plastic debris <5 mm), and concentrations of deposited molecules are orders of magnitude lower than in typical experiments. Here we address these issues by developing a toxin point-source model platform capable of probing molecular level toxin deposition, desorption, and restructuring in situ and in real time under various model environments.

This novel platform is used to investigate the deposition and desorption of NP on the surface of two plastics commonly found in aquatic environments, poly(styrene) (PS) and poly(ethylene terephthalate) (PET) (Figure 1). The deposition behavior of NP on these plastics is compared across two contrasting environmental regimes: the humid air space above a calm lake surface, and the dry air above land. Additionally, to test the *permanence* of NP deposition, the system is agitated through alternating exposure to clean air and moving water, modeling the transit of plastic debris through environmental compartments (e.g., bobbing at the water surface, etc.). The total mass of NP molecules stably deposited under model lake and land conditions is determined through in situ quartz crystal microbalance (QCM) measurements. The molecular ordering behaviors of NP at the microplastic surface is described with sum frequency generation (SFG) vibrational spectroscopy, an elegant analytical tool for studying the in situ deposition and ordering of toxins on plastics at a molecular level in real time.[36−38] Because an SFG process is forbidden in centrosymmetric materials but allowed at surfaces or interfaces where inversion symmetry is broken, it is truly surface sensitive and can be applied without disturbing our plastic surfaces at much lower detection limits (less than a monolayer) than most traditional spectroscopic techniques. Additionally, SFG generates information on molecular vibrational group ordering and/or orientation on surfaces, yielding insights into how molecules deposit and reorder during and after deposition processes.[39−46]

Through this multifaceted analytical approach, we generate a physical picture of the effects of surface structure, interfacial water content, and environmental factors on the quantity and structuring of NP molecules adsorbed and desorbed from plastic surfaces under model conditions. This study can inform ecotoxicological models that describe the fate of endocrine disrupting alkylphenols in the environment.

EXPERIMENTAL SECTION

Materials. Deuterated poly(styrene) PS-d_8 (M_w 198000; M_n 165000) and poly(ethylene terephthalate) PET-d_4 (M_v 72000; M_w/M_n broad) were obtained from Polymer Source Inc. (Dorval, QC Canada). Toluene ≥99.3% purity, 2-chlorophenol (99+%) and deuterium oxide (99.9% atom D) were obtained from Sigma-Aldrich (St. Louis, MO). 4-nonylphenol (analytical standard, technical mixture, CAS 84852−15−3, 12 isomers) was purchased from Fluka (St. Louis, MO). All chemical materials were used as received.

Sample Preparation. Right angle calcium fluoride prisms (Altos Photonics) were used for SFG measurements and 10 MHz quartz crystals, etched surface, Au electrode (International Crystal Manufacturing) were used for QCM experiments (further details in the Supporting Information (SI)).

Polymers were dissolved in appropriate solvents in glass vials to prepare the plastic thin films on substrates. 1.5 wt % solutions of PS-d_8 were prepared with toluene and 1.5 wt % PET-d_4 solutions with 2-chlorophenol. Solutions were mixed using a vortex mixer (Vortex-Genie 2T, Scientific Industries Inc.) until clear. A P-6000 spin coater (Speedline Technologies) was used to prepare all plastic films. Samples were spin coated at 3000 rpm for 30 s on calcium fluoride prisms for SFG experiments and at 1500 rpm for 30 s on quartz crystals for QCM experiments. All films were prepared 1 day prior to experiments. After substrates were prepared, a stream of N_2 was applied for 3−5 min to help remove trapped solvent. Prepared substrates were then placed in a clean Petri dish purged with N_2 in a chemical hood overnight. The day of SFG or QCM experiments, N_2 was again applied to plastic films for 2−3 min to ensure solvent removal. Deuterated polymers were utilized to avoid spectral overlap of toxin and plastic signals for SFG experiments, and the same polymers were utilized for QCM experiments for consistency.

SFG Experiments. SFG has been widely applied to gather molecular-level information on a variety of surfaces and interfaces such as plastics exposed to model environmental conditions and in aqueous environments.[36−38,47−50] The SFG experiments conducted here were taken using ssp (s-polarized

DOI: 10.1021/acs.est.5b05598
Environ. Sci. Technol. 2016, 50, 1304−1312

signal, s-polarized 532 nm input beam and p-polarized tunable frequency IR input beam) and ppp polarization combinations. The surface area of analysis was approximately 0.19 mm^2, ideal to model the appropriate surface area of a microplastic. Details regarding SFG theory and setup have been extensively outlined in previous papers[51,52] and additional contextual information can be found in the SI.

Model Deposition of Nonylphenol on Plastics Under Dry Environments. Prisms were placed inside a sealed custom-made sample chamber at ambient conditions (design details in the SI). To test the deposition of gas-phase NP (NP(g)) on polystyrene plastic under "dry" conditions, three droplets of NP (~50 μL) were added to the bottom of the chamber 3 mm directly underneath the PS-d_8 plastic film. The NP was spread across the bottom with a sterile needle to an area of ~1 cm^2. Under such conditions, the maximum vapor concentration of NP at 25 °C would be about 1 ppm.

The experiment consisted of four steps (Figure 2): 1. The plastic was exposed to NP for 2.5 h; 2. The plastic was exposed to clean air for 1 h; 3. The plastic was exposed to moving water for 0.5 h (only ssp spectra obtained at this step due to time constraints); 4. The plastic was re-exposed to clean air for 1h. The details regarding these exposures are outlined in the SI. SFG spectra were obtained in situ in all conditions. SFG experiments to test the deposition of NP on PET-d_4 plastic surfaces were performed as above except only steps 1 and 2 were completed. All experiments were conducted with room humidity at 19–21% and temperature at 22–23 °C.

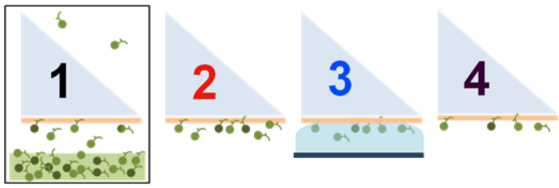

Figure 2. SFG experimental setup: 1. Plastic surface (tan line) attached to the bottom of an optical prism is introduced to the source of neat NP or NP/D_2O for 2.5 h (step 1 is highlighted in later SFG spectra as a black outline); 2. Plastic is exposed to clean air for 1 h (red-orange); 3. To agitate system, plastic is contacted to D_2O stirred at 125 rpm for 30 min (blue); 4. Plastic is re-exposed to air for 1 h (plum).

Model Deposition of NP on Plastics Under Humid Environments. SFG experiments for the NP(g) deposition on PS-d_8 and PET-d_4 under humid conditions were completed in an identical manner to the dry conditions experiments, except the pure NP droplets were substituted with 3 mL of a supersaturated 100 ppm mixture of NP in D_2O. The plastic film was placed 3 mm above the toxin source (water surface). Under these humid model conditions, the maximum concentration of NP was estimated to be much lower (~9 ppt at 25 °C) according to Raoult's Law for mixtures.

QCM Experiments. To determine the mass of NP molecules deposited on PS-d_8 under both dry and humid situations, QCM experiments were conducted in a similar manner to steps 1–2 of SFG experiments (Figure 2) using a custom-made crystal holder placed in the experimental chamber. Baseline QCM frequencies were measured in lab air prior to toxin introduction. QCM measurements were obtained in situ with the plastic-coated quartz crystals held 3 mm above pure NP or 100 ppm of NP solutions for 3 h and then exposed to clean air for ~20 min. QCM data were normalized to the theoretical mass deposited on the surface area of a plastic film utilized in the SFG experiments (depiction of a large microplastic). Further experimental details can be found in the SI.

RESULTS AND DISCUSSION

QCM Studies of NP and D_2O Deposition on PS. QCM experiments were performed to estimate the mass deposited on PS-d_8 plastic under model dry and humid conditions. Representative QCM mass deposition and desorption curves can be found in Figure 3. As expected, the QCM mass deposition curve for NP deposited on PS-d_8 under dry conditions (Figure 3a) illustrates a monotonic increase in mass deposited on the plastic. At 2.5 h, when the plastic would be exposed to clean air in SFG experiments, QCM results demonstrate approximately 195 ng of NP was deposited on a plastic with a surface area of 1.62 cm^2. Repeated experiments reveal total NP mass deposited on PS under dry conditions varied from 136 to 213 ng. Both QCM and SFG results (described below) indicate a constant rate of deposition from start to 2.5 h. To correctly interpret SFG spectra, the deposited masses calculated from QCM experiments must be compared to the mass of an NP monolayer (calculated ~170 ng). Therefore, the deposited mass of NP on PS under dry conditions varied from slightly under to slightly greater than the calculated monolayer of NP molecules.

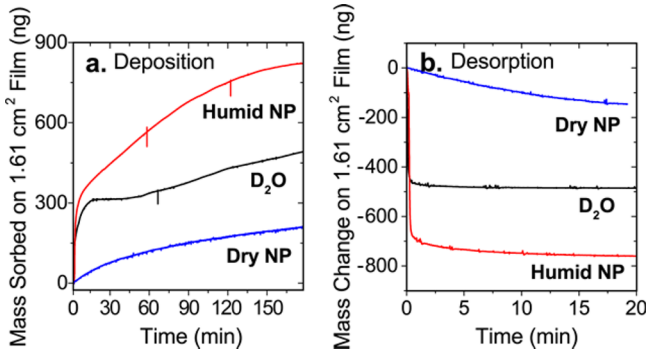

Figure 3. a. QCM curves of mass deposition on PS-d_8: NP only under dry conditions (blue); D_2O only under humid conditions (black); NP under humid conditions (red); 3b. Corresponding QCM curves of mass desorption once the three systems are exposed to clean air: Dry NP (blue), water (black), humid NP (red).

More importantly, every mass sorption/desorption curve collected under dry conditions reveal that much less than a monolayer of NP molecules remained on the plastic surface after the point source was removed and the plastic exposed to clean air for ~20 min (the sorption and desorption curve shown in Figure 3b is from one sample). The difference between sorbed and desorbed masses (Figure 3a/3b) indicates approximately 65 ng of NP remained on the plastic after 20 min of clean air exposure. Repeated experiments showed a stabilized mass deposited from 19 to 65 ng.

Comparatively, the sorption of D_2O only on PS (Figure 3a) is not monotonic, and consists of a very rapid initial increase and a plateau followed by a slower increase toward equilibrium (Figure 3a). Because we were modeling an NP point source rather than a system at vapor equilibrium, our QCM measurements were representations of both adsorption and

DOI: 10.1021/acs.est.5b05598
Environ. Sci. Technol. 2016, 50, 1304–1312

evaporation of molecules from the plastic surface. Such a case includes many factors: the evaporation rate of D_2O from the bulk source, the partitioning of D_2O into the PS-d_8 film, and the equilibrium between surface sorption and desorption. The initial rapid mass increase is attributed to the large vapor phase concentration difference between the ambient air (19% humidity) and the sealed chamber. The slower approach to equilibrium was likely dependent on the evaporation of D_2O and the equilibrium between the vapor phase D_2O and the film. Virtually no water was left in/on the plastic once the system was exposed to dry air for 20 min regardless of total mass sorbed. In fact, most of the D_2O desorbed within the first minute of exposure to dry room air. Repeated experiments revealed a varying mass of D_2O deposited from 500 to 1005 ng, which likely occurred due to slight changes in humidity and plastic surface dryness. Theoretical calculations determined the D_2O monolayer to weigh 1230 ng at minimum, so less than a monolayer of water was deposited during this time.

The QCM curve generated when NP was deposited on PS-d_8 under humid conditions is smooth and does not demonstrate the rate changes observed with D_2O deposition alone. Total mass deposited varied from 330 to 824 ng, statistically indistinguishable from the runs of D_2O only. This again is attributed to small changes in room humidity affecting the mass of water deposited on a given experiment. More important is the result from the humid/NP desorption curve (Figure 3b). After 20 min of air exposure approximately 62 ng of mass remained on the plastic. Regardless of the initial mass deposited, the mass remaining on 1.61 cm^2 of plastic after 20 min of drying was similar, varying from 33 to 62 ng. Normalizing the QCM results to the probing area of SFG experiments, modeling a small microplastic (0.19 mm^2), between 2 and 8 ng of NP was stably deposited under both model conditions.

Even though NP was present in ppt concentrations under humid conditions rather than ppm concentrations calculated in the absence of D_2O, similar masses remained on the plastics after sorption/desorption. This result was unexpected, given the much lower number of available NP molecules in the former case. But these results indicate that enough mass of NP was deposited under both conditions such that an equilibrium concentration of NP in/on PS was reached in ambient air.

SFG Studies on NP Adsorption/Desorption on PS Under Dry Conditions. SFG experiments were completed to model molecular surface changes on PS microplastics (probing area 0.19 mm^2) exposed to an NP point source under dry, warm (22−23 °C) conditions. SFG time-dependent ssp signals from NP at 2875 cm^{-1} (CH_3 (s)) and 3030 cm^{-1} (C−H stretching of the phenyl ring v_{20b} mode) were obtained during exposure of PS-d_8 to NP in air for 2 h (Figure 4a).

With increasing time the $CH_3(s)$ signal increases steadily, akin to a gas-phase mass deposition curve, indicating a consistent rate of NP deposition in agreement with QCM results. The SFG phenyl signal remains low in intensity and only slightly increases, suggesting that the phenyl rings are highly disordered during the deposition process. After approximately 1.75 h the $CH_3(s)$ and phenyl signal intensities remain similar, indicating a stabilized surface structure.

Two hours into the NP deposition, ssp and ppp SFG spectra were obtained in the chamber (Figure 4b) to determine NP structural information. After 2 h, QCM results indicated that more than a monolayer of NP molecules may be present on the plastic under both models. Therefore, quantitative calculations

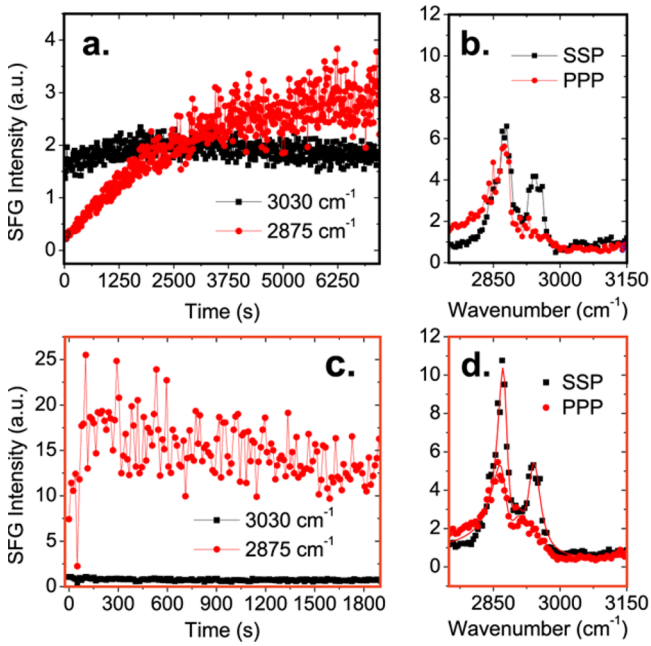

Figure 4. SFG results: 4a. Time dependent ssp signals detected at fixed frequencies 2875 and 3030 cm^{-1} during NP deposition process on PS-d_8 in dry chamber; 4b. The ssp and ppp spectra obtained after 2 h of exposure in chamber; 4c. Time dependent fixed frequency ssp signals obtained once chamber is removed; 4d. The ssp and ppp spectra obtained after 40 min of exposure to clean air with fits shown as red lines and data as points.

regarding NP functional group orientations may not accurately reflect molecular surface group behaviors. SFG spectra can reveal, however, how the NP molecules generally order on the PS surface with NP gas-phase molecules present in air. The spectra contain strong CH_3 peaks but very weak phenyl signal, indicating that during the deposition process the CH_3 groups on NPs are generally ordered but the NP phenol rings lay flat on the plastic surface or are disordered.

After 2.5 h of NP exposure, the point source of NP was removed and the plastic surface was exposed to clean air for 1 h. Figure 4c shows the time-dependent SFG signals of this process. The initial decrease in intensity, due to removal of the chamber and temporary blocking of laser beams, is followed by a dramatic increase in intensity (note intensity (I) of 25 (4c) versus 4 (4a) in the chamber). While a small percentage of the signal increase is due to the removal of quartz windows, the remaining increase originates from molecular reordering as the NP CH_3 groups stand up more toward the hydrophobic air surface upon exposure to clean air. Decreases in signal with increased air exposure time can be associated with the loss of surface molecules through evaporation (as shown in QCM results). Since SFG intensity is not linearly related to the number of the surface/interfacial molecules, but rather to both the number (the square of the number) and the orientation of surface/interfacial molecules, we cannot quantitatively compare the SFG and the QCM data, but their trends in changes are similar.

SFG signals indicate a stable surface structure at ∼30 min, when methyl and phenyl signals remain constant. By this time, enough surface NP molecules leave to yield a stable, ordered submonolayer of NP. SFG spectra obtained after 40 min of clean air exposure demonstrate clear $CH_3(s)$ and corresponding Fermi resonance signals. SFG calculations (in the SI) reveal the

DOI: 10.1021/acs.est.5b05598
Environ. Sci. Technol. 2016, 50, 1304−1312

$CH_3(s)$ groups order with an average tilt angle of 44° to the surface normal. This number is designated an average since the dozen isomers of NP will likely yield multiple CH_3 orientations. Thus, after clean air exposure, NP molecules are oriented such that phenol rings lie flat (or are disordered) on the plastic and CH_3 groups point toward the air.

To further test the stability of the deposited NP molecules, the plastic was exposed to moving water for 30 min (D_2O stirred at 125 rpm), and SFG time-dependent signals were obtained in situ (Figure 5a). A decrease in $CH_3(s)$ intensity

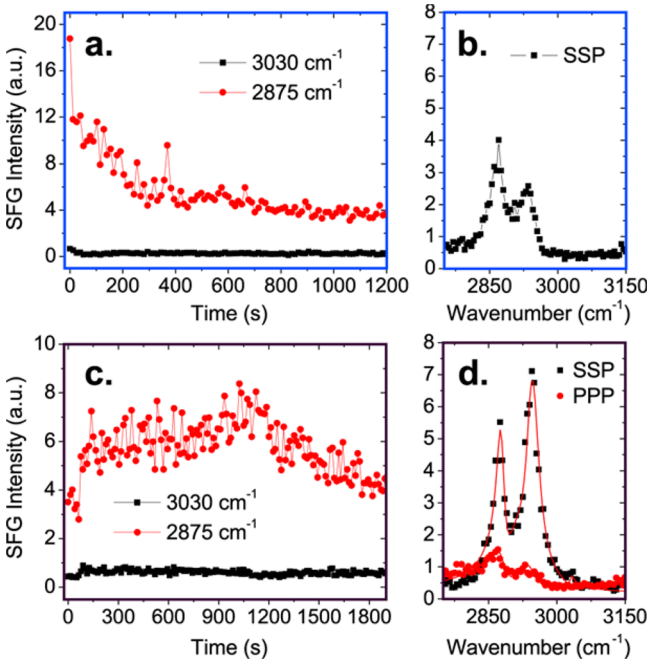

Figure 5. SFG results: 5a. Time dependent ssp signals detected at fixed frequencies 2875 and 3030 cm^{-1} during contact of PS-d_8 with NP to D_2O; 5b. The ssp spectra obtained after 20 min in D_2O; 5c. Time dependent fixed frequency ssp signals obtained after plastic was removed from D_2O; 5d. The ssp and ppp spectra obtained after 40 min of exposure to clean air with fits shown as red lines and data as points.

occurred quickly, from both loss of molecules and increased disorder. At 20 min of water contact, SFG ssp spectra show CH_3 and CH_2 groups remained somewhat ordered at the water interface (Figure 5b).

Next, the plastic was re-exposed to air for 1 h. Fewer surface NP molecules likely remained as evidenced by the decrease in intensity of the $CH_3(s)$ peak in Figure 5d compared to Figure 4d and the overall decrease in intensity of time dependent signals in air (Figure 5c). Fitting results of spectra in Figure 5d demonstrate that the methyl groups tilt at an average of 43° to the surface normal, similar to their calculation in air before water contact. The lack of large phenyl signal indicates that the phenol rings lay down or were disordered. Most importantly, even after agitating steps modeling an environmental plastic desbris re-exposed to moving water, some NP molecules persisted on the plastic surface.

SFG Studies on NP Adsorption/Desorption on PS Under Humid Conditions. SFG experiments were completed to model molecular surface changes on PS microplastics exposed to an NP point source under humid conditions like those near a body of fresh water. SFG time-dependent signals obtained during NP deposition demonstrate an interesting trend in signal intensities (Figure 6a). An increase and decrease

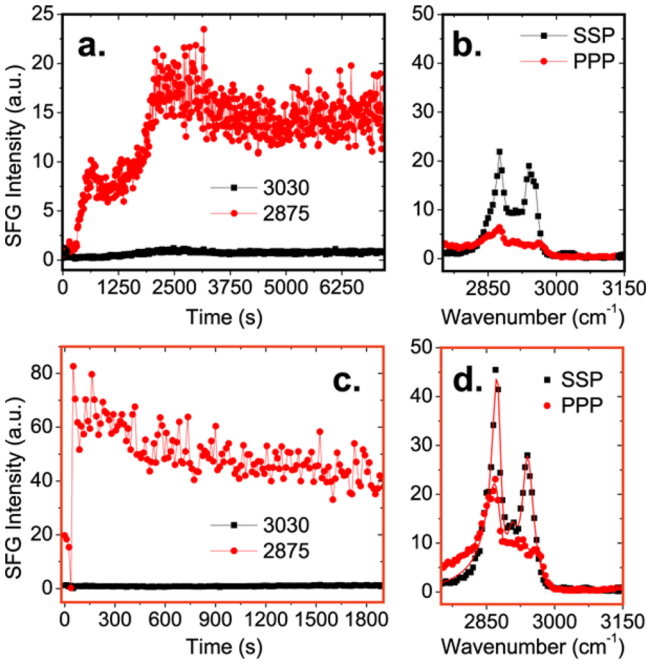

Figure 6. SFG results: 6a. Time dependent ssp signals detected at fixed frequencies 2875 and 3030 cm^{-1} during the NP deposition process on PS-d_8 in humid chamber; 6b. The ssp and ppp spectra obtained after 2 h of exposure in chamber; 6c. Time dependent fixed frequency ssp signals obtained once chamber is removed; 6d. The ssp and ppp spectra obtained after 40 min of exposure to clean air with fits shown as red lines and data as points.

in intensity of the $CH_3(s)$ signal were observed around 700 and 2400 s. Additionally, the $CH_3(s)$ signal is of a much higher intensity than in the dry condition model (note maximum I of 20 versus 3.5). Only minute changes in the phenyl ring signal were observed as an increase and decrease around 2500 s.

At 2 h of exposure, ssp and ppp SFG spectra were obtained inside the deposition chamber (Figure 6b). Here, NP CH_3 signals are present under both polarizations, indicating methyl group ordering. From a purely qualitative perspective, if water molecules were present on/near the surface of the plastic, the rearrangement of CH_3 groups away from the surface is likely.

Spectra appeared similar to those in the low humidity model once the plastic was exposed to clean air (Figure 6c). A clear initial signal increase and decrease was observed for the $CH_3(s)$ group as the chamber was removed and NP molecules evaporated. After 30 min, SFG signals remained similar in intensity. NP SFG signals were much higher after exposure to air for 1 h in the humid model than the dry land model, which may be indicative of better molecular ordering on the surface of the plastic exposed to a humid NP-source environment.

After 40 min of clean air exposure, SFG spectra were obtained from surface NP molecules (Figure 6d). Calculations revealed the CH_3 molecular groups tilted at an average of 44° to the surface normal, very similar to the calculated orientation of CH_3 groups 40 min after NP deposition under dry conditions. Interestingly, the overall SFG signal intensities were still much higher after the humid deposition compared to the dry deposition. Normally an increase in SFG intensity with no evidence of molecular orientation change may be attributed

DOI: 10.1021/acs.est.5b05598
Environ. Sci. Technol. 2016, 50, 1304−1312

to an increased number of functional groups at an interface. However, QCM results indicated a similar number of NP molecules remained on the plastic surface after 20 min of exposure to clean air, regardless of deposition environment.

Here, it is believed the presence of water on/near the plastic played a role in the increased SFG signal intensities. Under the dry land model it is likely the deposited NP molecules originating from multiple isomers yielded a broad surface orientation distribution. Even though the calculated average orientation of methyl groups was 44°, the SFG signal did not originate from all surface NP methyl groups. SFG signals from methyl groups pointing in opposite directions (inward versus outward from the surface) are canceled out. This results in decreased SFG methyl signal intensities. Under the humid model, water present during the deposition process could form a more hydrophilic plastic surface (water evidence discussed in the SI) and more hydrophobic methyl groups from the dozen NP isomers tilted away from the plastic surface. In other words, more methyl groups order on the surface in similar directions, generating much stronger SFG signals. Thus, even though there were no major changes in average calculated methyl orientation after the NP is deposited in a freshwater model environment compared to the dry land model, a change in methyl signal intensities can be reasonably attributed to increased NP ordering under humid conditions.

Upon exposure to the agitating water system, $CH_3(s)$ signals dropped dramatically, (Figure 7a and b) but increased once the plastic is re-exposed to air and reached a stable surface structure after 30 min (Figure 7c and d). Owing to a loss of surface molecules, the SFG signals were much lower than first exposure to air, and $CH_3(s)$ groups are still well ordered, with an average orientation of 33° to the surface normal after more than 40 min

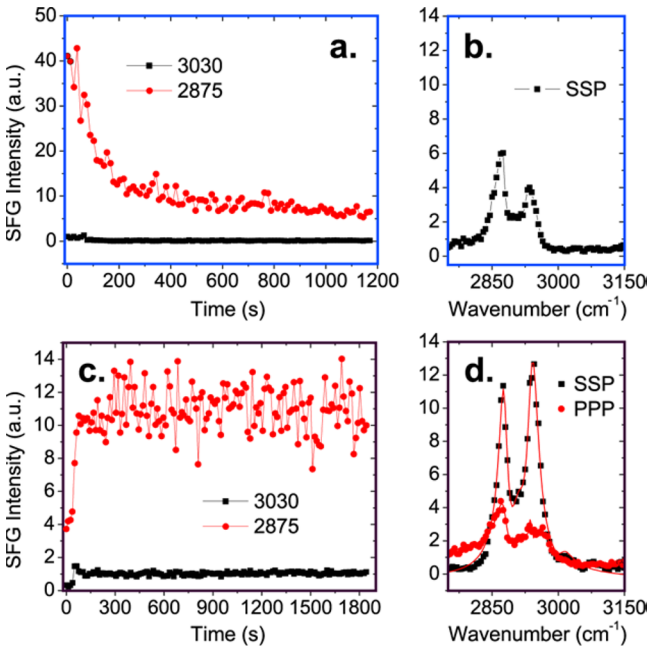

Figure 7. SFG results: 7a. Time dependent ssp signals detected at fixed frequencies 2875 and 3030 cm^{-1} during contact of PS-d_8 with NP to D_2O; 7b. The ssp spectrum obtained after 20 min in D_2O; 7c. Time dependent fixed frequency ssp signals obtained after plastic was removed from D_2O; 7d. The ssp and ppp spectra obtained after 40 min of exposure to clean air with fits shown as red lines and data as points.

of drying. This indicates that the NP molecules adopted different orientations at equilibrium after deposition under humid conditions compared to dry conditions. This data also confirms that NP molecules remained on the plastic surface after agitation.

Further SFG experiments were performed to investigate the origins of $CH_3(s)$ NP signal fluctuation during humid deposition. One plausible source was variation the amount and/or degree of ordered water on the plastic surface. Therefore, SFG data was obtained of ordered water at the PS/air interface during NP deposition under the humid model (SI Figure S-3a). While QCM data and ATR-FTIR data (SI Figure S-5) indicate a steady deposition of water molecules during the humid NP deposition, the SFG signals obtained of ordered water did not change over NP deposition time (SI Figure S-3a). Consequently we cannot appoint the degree of water ordering as the underlying root for SFG methyl signal aberration during humid NP deposition. We can reasonably conclude that the increased presence of interfacial water molecules induces changes resulting in SFG signal fluctuations since the major difference between the two deposition models is the increased number of water molecules (and decreased numbers of NP). It is likely that hydrophobic/hydrophilic interactions between the plastic, NPs and water contributed to SFG $CH_3(s)$ signal changes but a more detailed investigation into the physical mechanism behind the SFG signal fluctuation should be conducted in the future. Interestingly, the same $CH_3(s)$ signal fluctuation trend was found during humid NP deposition on PS using NP-spiked water collected from Lake Erie in place of D_2O, demonstrating that this NP ordering phenomenon occurred in a realistic simulation of plastic debris in the Great Lakes (SI Figure S-4).

SFG Studies on NP Adsorption/Desorption on PET Under Dry and Humid Conditions. SFG spectra were obtained during and after the deposition process of NP on PET-d_4 under dry and humid conditions to compare the effect of plastic surfaces on NP deposition behaviors. The deposition of NP on PET in dry land conditions yielded much faster initial $CH_3(s)$ signal increases, slight signal fluctuation, and a slightly higher signal than deposition on PS (Figure 8a). Thus, the plastic surface influenced how NP molecules deposited under these conditions. PET, a more hydrophilic plastic than PS, will contain some surface-bound water molecules even under low humidity conditions. These molecules may affect NP ordering during deposition, similar to observations with PS under humidity. Once the plastic was exposed to air after deposition, some loss of NP was observed (Figure 8b).

Deposition of NP on PET under humid conditions resulted in lower NP SFG signal intensity compared to PS under humidity and PET under dry conditions. Increases in $CH_3(s)$ signal fluctuation were observed with initial rate of signal increase occurring more quickly on the PET surface compared to PS (Figure 8c). NP loss was observed after removal of the chamber (Figure 8d). We can conclude that NP molecular groups reordered in a similar pattern under humid conditions on multiple plastics, although greatly increased ordering was not observed on PET under humid conditions, likely because the PET surface became too hydrophilic to induce a favorable NP deposition environment. Therefore, a humid model lake environment can induce unique NP molecular rearrangement, but may not always increase the ordering of NP molecules deposited on a plastic.

DOI: 10.1021/acs.est.5b05598
Environ. Sci. Technol. 2016, 50, 1304−1312

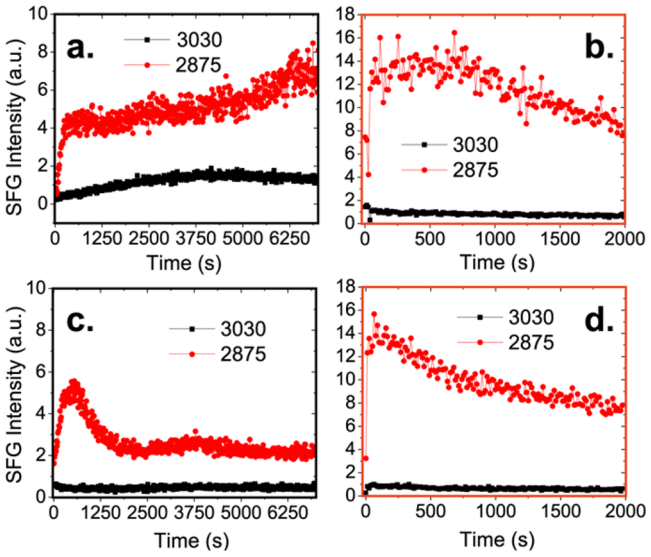

Figure 8. SFG signals detected at fixed frequencies 2875 and 3030 cm^{-1}: 8a. Time dependent ssp signals during NP deposition process on PET-d_4 in dry chamber; 8b. Time dependent ssp signals obtained once chamber was removed; 8c. Time dependent ssp signals during NP deposition process on PET-d_4 in humid chamber; 8d. Time dependent ssp signals obtained once chamber was removed.

Presence of Water Vapor Induces Deposition Changes. Model in situ deposition experiments revealed that Laurentain Great Lakes ecological toxin NP quickly deposits on hydrophobic microplastics under dry land and air/surface lake microlayer conditions. Surprisingly, a similar number of stable NP molecules (2−8 ng) were deposited on a model small PS microplastic under both environments despite vast differences in initial NP vapor concentration. After initial deposition in the two models, agitating conditions (moving water and re-exposure to air) removed NP molecules from PS, but some surface NP remained regardless of further changes in environment.

NP molecules deposited and reordered in a unique manner during deposition on hydrophobic plastics in the lake model (using D_2O or Lake Erie water, experiment in the SI). The initial environment during NP deposition dictated the amount of NP surface ordering on PS throughout all testing stages. NP surface methyl groups originally deposited under humidity remained much more ordered on PS than those of NP molecules deposited under dry conditions.

Environmental Implications. Our low-volatility model demonstrated capability to probe the deposition and desorption processes of alkylphenols under different conditions and holds promise to model more complicated environments hosting point-source toxins. Results indicate that the prolific toxin nonylphenol may quickly and semipermanently deposit on virgin hydrophobic microplastics floating on a lake surface under extremely low air concentrations (lower than 9 ppt) and calm weather conditions. In the case of PS, there is great potential for just as much NP to sorb and collect on plastic in a humid environment compared to a dry one with a much higher concentration of gas-phase NPs. If NP or similar environmental toxins deposit on hydrophobic microplastics in a freshwater system, it is highly likely that some toxins will remain in the surface layers of the plastic (and not sorb completely into the plastic) until transfer to a more favorable amphiphilic environment is available. Over the next decade, the input of plastic debris to aquatic systems is projected to increase by an order of magnitude;[53] an improved understanding of interactions between plastics, toxins, and inhabitants is of paramount importance as we build a framework to assess the impacts of plastic pollution on ecosystem health.

■ ASSOCIATED CONTENT

Supporting Information

The Supporting Information is available free of charge on the ACS Publications website at DOI: 10.1021/acs.est.5b05598.

Expanded SFG experimental information, additional SFG data and calculations, QCM 444 information, and ATR-FTIR experimental data (PDF)

■ AUTHOR INFORMATION

Corresponding Authors

*(Z.C.) Phone: (734) 615-4189; e-mail: zhanc@umich.edu.

*(M.D.) Phone: (734) 764-6219; e-mail: duhaimem@umich.edu.

Notes

The authors declare no competing financial interest.

■ ACKNOWLEDGMENTS

This research is supported by the University of Michigan Water Center and the Fred A. and Barbara M. Erb Family Foundation. We thank Roy Wentz at the University of Michigan Chemistry glass shop for his aid in design and fabrication of the sample chamber.

■ REFERENCES

(1) Eriksen, M.; Mason, S.; Wilson, S.; Box, C.; Zellers, A.; Edwards, W.; Farley, H.; Amato, S. Microplastic pollution in the surface waters of the Laurentian Great Lakes. *Mar. Pollut. Bull.* **2013**, *77*, 177−182.

(2) Free, C. M.; Jensen, O. P.; Mason, S. A.; Eriksen, M.; Williamson, N. J.; Boldgiv, B. High-levels of microplastic pollution in a large, remote, mountain lake. *Mar. Pollut. Bull.* **2014**, *85*, 156−163.

(3) McCormick, A.; Hoellein, T. J.; Mason, S. A.; Schluep, J.; Kelly, J. J. Microplastic is an Abundant and Distinct Microbial Habitat in an Urban River. *Environ. Sci. Technol.* **2014**, *48*, 11863−11871.

(4) Gregory, M. Environmental implications of plastic debris in marine settings- entanglement, ingestion, smothering, hangers-on, hitch-hiking and alien invasions. *Philos. Trans. R. Soc., B* **2009**, *364*, 2013−2025.

(5) Rios, L.; Moore, C.; Jones, P. Persistent organic pollutants carried by synthetic polymers in the ocean environment. *Mar. Pollut. Bull.* **2007**, *54*, 1230−1237.

(6) Teuten, E.; Rowland, S.; Galloway, T.; Thompson, R. Potential for plastics to transport hydrophobic contaminants. *Environ. Sci. Technol.* **2007**, *41*, 7759−7764.

(7) Frias, J. P. G. L.; Sobral, P.; Ferreira, A. M. Organic pollutants in microplastics from two beaches of the Portuguese coast. *Mar. Pollut. Bull.* **2010**, *60*, 1988−1992.

(8) Teuten, E.; Saquing, J.; Knappe, D.; Barlaz, M.; Jonsson, S.; Bjorn, A.; Rowland, S.; Thompson, R.; Galloway, T.; Yamashita, R.; Ochi, D.; Watanuki, Y.; Moore, C.; Viet, P.; Tana, T.; Prudente, M.; Boonyatumanond, R.; Zakaria, M.; Akkhavong, K.; Ogata, Y.; Hirai, H.; Iwasa, S.; Mizukawa, K.; Hagino, Y.; Imamura, A.; Saha, M.; Takada, H. Transport and release of chemicals from plastics to the environment and to wildlife. *Philos. Trans. R. Soc., B* **2009**, *364*, 2027−2045.

(9) Cole, M.; Lindeque, P.; Halsband, C.; Galloway, T. S. Microplastics as contaminants in the marine environment: A review. *Mar. Pollut. Bull.* **2011**, *62*, 2588−2597.

DOI: 10.1021/acs.est.5b05598
Environ. Sci. Technol. 2016, 50, 1304−1312

(10) Wurl, O.; Obbard, J. P. A review of pollutants in the sea-surface microlayer (SML): a unique habitat for marine organisms. *Mar. Pollut. Bull.* **2004**, *48*, 1016−1030.
(11) Mato, Y.; Isobe, T.; Takada, H.; Kanehiro, H.; Ohtake, C.; Kaminuma, T. Plastic resin pellets as a transport medium for toxic chemicals in the marine environment. *Environ. Sci. Technol.* **2001**, *35*, 318−324.
(12) Bakir, A.; Rowland, S.; Thompson, R. Enhanced desorption of persistent organic pollutants from microplastics under simulated physiological conditions. *Environ. Pollut.* **2013**, *185C*, 16−23.
(13) Bennie, D. T.; Sullivan, C. A.; Lee, H. B.; Peart, T. E.; Maguire, R. J. Occurrence of alkylphenols and alkylphenol mono- and diethoxylates in natural waters of the Laurentian Great Lakes basin and the upper St. Lawrence River. *Sci. Total Environ.* **1997**, *193*, 263−275.
(14) Li, H.; Helm, P. A.; Metcalfe, C. D. Sampling in the Great Lakes for pharmaceuticals, personal care products, and endocrine-disrupting substances using the passive polar organic chemical integrative sampler. *Environ. Toxicol. Chem.* **2010**, *29*, 751−762.
(15) Bennett, E. R.; Metcalfe, C. D. Distribution of degradation products of alkylphenol ethoxylates near sewage treatment plants in the lower Great Lakes, North America. *Environ. Toxicol. Chem.* **2000**, *19*, 784−792.
(16) Kavanagh, R. J.; Balch, G. C.; Kiparissis, Y.; Niimi, A. J.; Sherry, J.; Tinson, C.; Metcalfe, C. D. Endocrine disruption and altered gonadal development in white perch (Morone americana) from the lower Great Lakes region. *Environ. Health Perspect.* **2004**, *112*, 898−902.
(17) Dachs, J.; Van Ry, D. A.; Eisenreich, S. J. Occurrence of Estrogenic Nonylphenols in the Urban and Coastal Atmosphere of the Lower Hudson River Estuary. *Environ. Sci. Technol.* **1999**, *33*, 2676−2679.
(18) Castañeda, R. A.; Avlijas, S.; Simard, M. A.; Ricciardi, A. Microplastic pollution in St. Lawrence River sediments. *Can. J. Fish. Aquat. Sci.* **2014**, *71*, 1767−1771.
(19) Gouin, T.; Roche, N.; Lohmann, R.; Hodges, G. A thermodynamic approach for assessing the environmental exposure of chemicals absorbed to microplastic. *Environ. Sci. Technol.* **2011**, *45*, 1466−1472.
(20) *Nonylphenol (NP) and Nonylphenol Ethoxylates (NPEs) Action Plan*, RIN 2070-ZA09; U.S. Environmental Protection Agency, 2010.
(21) *SVHC Support Document-4-Nonylphenol, Branched and Linear*; European Chemicals Agency, 2012.
(22) Soares, A.; Guieysse, B.; Jefferson, B.; Cartmell, E.; Lester, J. N. Nonylphenol in the environment: A critical review on occurrence, fate, toxicity and treatment in wastewaters. *Environ. Int.* **2008**, *34*, 1033−1049.
(23) Hung, Y. T.; Wang, L. K.; Shammas, N. K. *Handbook of Environment and Waste Management: Air and Water Pollution Control*; World Scientific, 2012.
(24) Lichtfouse, E.; Schwarzbauer, J.; Robert, D. *Environmental Chemistry: Green Chemistry and Pollutants in Ecosystems*; Springer, 2005.
(25) Giger, W.; Brunner, P.; Schaffner, C. 4-Nonylphenol in sewage sludge: accumulation of toxic metabolites from nonionic surfactants. *Science* **1984**, *225*, 623−625.
(26) Bidleman, T. F.; Renberg, L. Determination of vapor pressures for chloroguaiacols, chloroveratroles, and nonylphenol by gas chromatography. *Chemosphere* **1985**, *14*, 1475−1481.
(27) Ieda, T.; Horii, Y.; Petrick, G.; Yamashita, N.; Ochiai, N.; Kannan, K. Analysis of Nonylphenol Isomers in a Technical Mixture and in Water by Comprehensive Two-Dimensional Gas Chromatography−Mass Spectrometry. *Environ. Sci. Technol.* **2005**, *39*, 7202−7207.
(28) Addition of Nonylphenol Category; Community Right-To-Know Toxic Chemical Release Reporting. *Fed. Regist.* **2014**;, *79*, 58686−58693.
(29) Antunes, J.; Frias, J.; Micaelo, A.; Sobral, P. Resin pellets from beaches of the Portuguese coast and adsorbed persistent organic pollutants. *Estuarine, Coastal Shelf Sci.* **2013**, *130*, 62−69.
(30) Ivar do Sul, J.; Costa, M. The present and future of microplastic pollution in the marine environment. *Environ. Pollut.* **2014**, *185*, 352−364.
(31) Andrady, A. L. Microplastics in the marine environment. *Mar. Pollut. Bull.* **2011**, *62*, 1596−1605.
(32) Lorena Rios Mendoza, P. J. Characterization of Microplastics and Toxic Species Extracted from the Microplastic Samples from the North Pacific Gyre Collection Sites. *Environ. Chem.* **2015**, *12*, 611−617.
(33) Wagner, M.; Scherer, C.; Alvarez-Munoz, D.; Brennholt, N.; Bourrain, X.; Buchinger, S.; Fries, E.; Grosbois, C.; Klasmeier, J.; Marti, T.; Rodriguez-Mozaz, S.; Urbatzka, R.; Vethaak, A.; Winther-Nielsen, M.; Reifferscheid, G. Microplastics in freshwater ecosystems: what we know and what we need to know. *Environ. Sci. Eur.* **2014**, *26*, 12.
(34) Eerkes-Medrano, D.; Thompson, R. C.; Aldridge, D. C. Microplastics in freshwater systems: A review of the emerging threats, identification of knowledge gaps and prioritisation of research needs. *Water Res.* **2015**, *75*, 63−82.
(35) Morabito, P. L.; Ormand, J. R.; Nestrick, T. J. Dynamic Vapor Generator for Moderate and Low Volatility Compounds. *Chemosphere* **1990**, *21*, 991−997.
(36) Hankett, J. M.; Lu, X. L.; Liu, Y. W.; Seeley, E.; Chen, Z. Interfacial molecular restructuring of plasticized polymers in water. *Phys. Chem. Chem. Phys.* **2014**, *16*, 20097−20106.
(37) Hankett, J. M.; Zhang, C.; Chen, Z. Sum Frequency Generation and Coherent Anti-Stokes Raman Spectroscopic Studies on Plasma-Treated Plasticized Polyvinyl Chloride Films. *Langmuir* **2012**, *28*, 4654−4662.
(38) Zhang, X. X.; Li, Y. X.; Hankett, J. M.; Chen, Z. The molecular interfacial structure and plasticizer migration behavior of ″green″ plasticized poly(vinyl chloride). *Phys. Chem. Chem. Phys.* **2015**, *17*, 4472−4482.
(39) Lis, D.; Backus, E. H. G.; Hunger, J.; Parekh, S. H.; Bonn, M. Liquid flow along a solid surface reversibly alters interfacial chemistry. *Science* **2014**, *344*, 1138−1142.
(40) Wang, T.; Li, D. W.; Lu, X. L.; Khmaladze, A.; Han, X. F.; Ye, S. J.; Yang, P.; Xue, G.; He, N. Y.; Chen, Z. Single Lipid Bilayers Constructed on Polymer Cushion Studied by Sum Frequency Generation Vibrational Spectroscopy. *J. Phys. Chem. C* **2011**, *115*, 7613−7620.
(41) Stokes, G. Y.; Chen, E. H.; Walter, S. R.; Geiger, F. M. Two Reactivity Modes in the Heterogeneous Cyclohexene Ozonolysis under Tropospherically Relevant Ozone-Rich and Ozone-Limited Conditions. *J. Phys. Chem. A* **2009**, *113*, 8985−8993.
(42) Song, S. H.; Koelsch, P.; Weidner, T.; Wagner, M. S.; Castner, D. G. Sodium Dodecyl Sulfate Adsorption onto Positively Charged Surfaces: Mono layer Formation With Opposing Headgroup Orientations. *Langmuir* **2013**, *29*, 12710−12719.
(43) Kristalyn, C. B.; Watt, S.; Spanninga, S. A.; Barnard, R. A.; Nguyen, K.; Chen, Z. Investigation of sub-monolayer, monolayer, and multilayer self-assembled semifluorinated alkylsilane films. *J. Colloid Interface Sci.* **2011**, *353*, 322−330.
(44) Ebben, C. J.; Ault, A. P.; Ruppel, M. J.; Ryder, O. S.; Bertram, T. H.; Grassian, V. H.; Prather, K. A.; Geiger, F. M. Size-Resolved Sea Spray Aerosol Particles Studied by Vibrational Sum Frequency Generation. *J. Phys. Chem. A* **2013**, *117*, 6589−6601.
(45) Tian, K. Z.; Zhang, B. X.; Ye, S. J.; Luo, Y. Intermolecular Interactions at the Interface Quantified by Surface-Sensitive Second-Order Fermi Resonant Signals. *J. Phys. Chem. C* **2015**, *119*, 16587−16595.
(46) Ma, S. L.; Li, H. C.; Tian, K. Z.; Ye, S. J.; Luo, Y. In Situ and Real-Time SFG Measurements Revealing Organization and Transport of Cholesterol Analogue 6-Ketocholestanol in a Cell Membrane. *J. Phys. Chem. Lett.* **2014**, *5*, 419−424.

DOI: 10.1021/acs.est.5b05598
Environ. Sci. Technol. 2016, 50, 1304−1312

(47) Hankett, J. M.; Collin, W. R.; Chen, Z. Molecular Structural Changes of Plasticized PVC after UV Light Exposure. *J. Phys. Chem. B* **2013**, *117*, 16336−16344.
(48) Hankett, J. M.; Liu, Y. W.; Zhang, X. X.; Zhang, C.; Chen, Z. Molecular level studies of polymer behaviors at the water interface using sum frequency generation vibrational spectroscopy. *J. Polym. Sci., Part B: Polym. Phys.* **2013**, *51*, 311−328.
(49) Hsiao, E.; Barnette, A. L.; Bradley, L. C.; Kim, S. H. Hydrophobic but hygroscopic polymer films–identifying interfacial species and understanding water ingress behavior. *ACS Appl. Mater. Interfaces* **2011**, *3*, 4236−4241.
(50) Hu, D.; Yang, Z.; Chou, K. C. Interactions of Polyelectrolytes with Water and Ions at Air/Water Interfaces Studied by Phase-Sensitive Sum Frequency Generation Vibrational Spectroscopy. *J. Phys. Chem. C* **2013**, *117*, 15698−15703.
(51) Shen, Y. R. *The Principles of Nonlinear Optics*; Wiley: New York, 1984.
(52) Shen, Y. R. Surface-Properties Probed by 2nd-Harmonic and Sum-Frequency Generation. *Nature* **1989**, *337*, 519−525.
(53) Jambeck, J. R.; Geyer, R.; Wilcox, C.; Siegler, T. R.; Perryman, M.; Andrady, A.; Narayan, R.; Law, K. L. Plastic waste inputs from land into the ocean. *Science* **2015**, *347*, 768−771.

DOI: 10.1021/acs.est.5b05598
Environ. Sci. Technol. 2016, 50, 1304−1312